OBLIQUE IMPACT OF TWO CYLINDERS IN A UNIFORM FLOW

by
Zhi Guo and Allen T. Chwang

Sponsored by

Ocean Engineering Division
Office of Naval Research
Grant N00014-89-J-1581

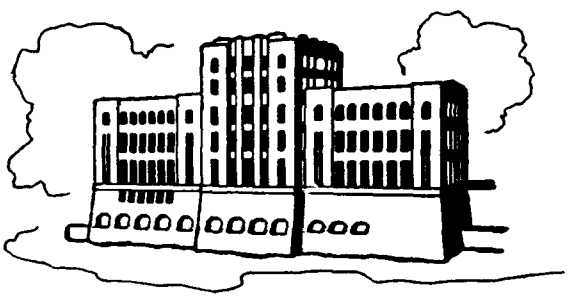

IIHR Report No. 333

Iowa Institute of Hydraulic Research
The University of Iowa
Iowa City, Iowa 52242

October 1989

OBLIQUE IMPACT OF TWO CYLINDERS IN A UNIFORM FLOW

by

Zhi Guo and Allen T. Chwang

Sponsored by

The Ocean Engineering Division
The Office of Naval Research
Under Grant N00014-89-J-1581

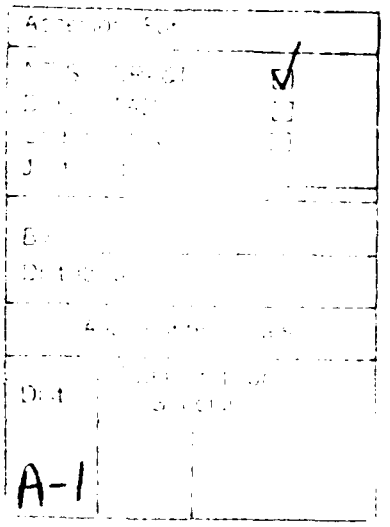

IIHR Report No. 333

Iowa Institute of Hydraulic Research
The University of Iowa
Iowa City, Iowa 52242

October 1989

Unclassified

SECURITY CLASSIFICATION OF THIS PAGE (When Data Entered)

REPORT DOCUMENTATION PAGE		READ INSTRUCTIONS BEFORE COMPLETING FORM
1. REPORT NUMBER IIHR Report No. 333	2. GOVT ACCESSION NO.	3. RECIPIENT'S CATALOG NUMBER
4. TITLE (and Subtitle) Oblique Impact of Two Cylinders in a Uniform Flow		5. TYPE OF REPORT & PERIOD COVERED Technical Report 2/1/89 - 10/31/89 6. PERFORMING ORG. REPORT NUMBER IIHR Report No. 333
7. AUTHOR(s) Zhi Guo and Allen T. Chwang		8. CONTRACT OR GRANT NUMBER(s) N00014-89-J-1581
9. PERFORMING ORGANIZATION NAME AND ADDRESS Iowa Institute of Hydraulic Research The University of Iowa Iowa City, Iowa 52242-1595		10. PROGRAM ELEMENT, PROJECT, TASK AREA & WORK UNIT NUMBERS
11. CONTROLLING OFFICE NAME AND ADDRESS The Ocean Engineering Division, The Office of Naval Research, 800 N Quincy Street, Arlington, Virginia 22217-5000		12. REPORT DATE October 1989 13. NUMBER OF PAGES 38
14. MONITORING AGENCY NAME & ADDRESS(if different from Controlling Office) Office of Naval Research Resident Representative, University of Washington, 315 University District Building, 1107 N. E. 45th Street, Seattle, Washington 98105-4631		15. SECURITY CLASS. (of this report) Unclassified 15a. DECLASSIFICATION/DOWNGRADING SCHEDULE

16. DISTRIBUTION STATEMENT (of this Report)

Approved for Public Release; Distribution Unlimited

17. DISTRIBUTION STATEMENT (of the abstract entered in Block 20, if different from Report)

Unlimited

18. SUPPLEMENTARY NOTES

19. KEY WORDS (Continue on reverse side if necessary and identify by block number)

Hydrodynamic Interactions, Oblique Impact, Particle Trajectories, Relative Motion of Two Cylinders, Potential-Flow Theory, Numerical Solution of Integral Equations.

20. ABSTRACT (Continue on reverse side if necessary and identify by block number)

The oblique motion of a circular cylinder through an inviscid and incompressible fluid, conveyed by a uniform flow at infinity, in the vicinity of another cylinder fixed in space is considered. In a relative polar coordinate system moving with the stream, the kinetic energy of the fluid is expressed as a function of six added masses due to motions parallel and perpendicular to the line joining the centers of the cylinder pair. The Lagrange's equations of motion are then integrated for the trajectories of the moving

DD FORM 1 JAN 73 1473 EDITION OF 1 NOV 65 IS OBSOLETE
S/N 0102-LF-014-6601

Unclassified

SECURITY CLASSIFICATION OF THIS PAGE (When Data Entered)

cylinder. In order to evaluate the added masses and their derivatives with respect to the separation distance between the cylinders in terms of the hydrodynamic singularities, the method of successive images, initiated by Hicks, and the Taylor's added-mass formula are applied, and analytic solutions in closed form are obtained thereafter. The dynamic behavior of a drifting body in the close proximity of a fixed one is investigated by considering the limiting values of the fluid kinetic energy and the interaction forces on each body. The reliability of the numerical approximation of added masses and their derivatives is also discussed in the present study. The integral equations, in terms of surface source distributions and their derivatives on both circles, are carefully modified for obtaining accurate numerical solutions.

TABLE OF CONTENTS

ABSTRACT

The oblique motion of a circular cylinder through an inviscid and incompressible fluid, conveyed by a uniform flow at infinity, in the vicinity of another cylinder fixed in space is considered. In a relative polar coordinate system moving with the stream, the kinetic energy of the fluid is expressed as a function of six added masses due to motions parallel and perpendicular to the line joining the centers of the cylinder pair. The Lagrange's equations of motion are then integrated for the trajectories of the moving cylinder. In order to evaluate the added masses and their derivatives with respect to the separation distance between the cylinders in terms of the hydrodynamic singularities, the method of successive images, initiated by Hicks[1], and the Taylor's added-mass formula are applied, and analytic solutions in closed form are obtained thereafter. The dynamic behavior of a drifting body in the close proximity of a fixed one is investigated by considering the limiting values of the fluid kinetic energy and the interaction forces on each body. The reliability of the numerical approximation of added masses and their derivatives is also discussed in the present study. The integral equations, in terms of surface source distributions and their derivatives on both circles, are carefully modified for obtaining accurate numerical solutions.

ACKNOWLEDGEMENTS

The authors wish to express their special thanks to Professor Lou Landweber for his helpful recommendations and suggestions. This work was sponsored by the Ocean Engineering Division, the Office of Naval Research, under Grant N00014-89-J-1581.

I. INTRODUCTION

The problem presented by motions of two or multiple solid bodies in an inviscid and incompressible fluid appears in many research fields. For example, the determination of hydrodynamic interactions between an offshore structure and floating ice masses is one of the practical problems in the oil industry. The prediction of the amount of liquid droplets, which are conveyed by the air flow and collected by a solid surface, is important in the atmospheric icing research. In all cases concerned, the Reynolds number, which is the ratio of the inertia effect to the viscous effect, is fairly large such that the potential-flow theory is reasonably applicable.

One and half centuries ago, Hicks[1] first considered motions of two circular cylinders moving in any manner in an unbounded fluid. He studied the velocity potential due to the distribution of unit sources spread over each surface which was first assumed to be stationary, and then found the velocity potential due to the motion of two cylinders by proportionating the magnitude of each source to the normal motion of the surfaces. His method may be too complicated to be applied in such cases where the main concern is the motion of solids only. A general framework for the motion of solids in an inviscid fluid was presented by Lamb[2]. He applied the Lagrange's equations of motion in generalized coordinates to the hydrodynamic interaction problem and related the fluid inertia to the equations of motion by virtue of the kinetic energy of the fluid. As an example, he considered one sphere approaching another along their centerline in a uniform flow. Yamamoto[3] and Isaacson & Cheung[4] obtained analytical and numerical solutions for forces on a pair of cylinders. Yamamoto[3] represented the complex potential field in terms of an infinite series of doublets by the method of successive images, which was first introduced by Hicks[5] for the motion of a pair of spheres. Yamamoto also derived a formula for forces, with some mistakes[6], on each cylinder based on the Blasius theorem. Isaacson & Cheung[4] did the same work numerically and their results agreed very well. However, their derivations about forces on solids may hardly be generalized to the three-dimensional problems because of the invalidity of the Blasius theorem. A better way of describing the motion of solids would be to use the Lagrange's equations of motion and to evaluate the

hydrodynamic interactions, in terms of added masses, by means of the generalized Taylor's added-mass formula. The application of the method of successive images is limited to certain symmetric geometries such as a pair of spheres or circular cylinders, due to its dependence on internal isolated singularities which cannot be found in general. Landweber and Chwang[7] developed a general formula and a numerical model, based on the boundary integral method, to obtain the added masses and added moments of inertia by solving the unknown source distributions on solid surfaces. When two bodies are not quite close to each other, their method gives good numerical results on added masses for various geometries. However, this technique depends on the simultaneous solution of a set of Fredholm integral equations of the second kind which may cause certain inaccuracy when the bodies are very close. There is room for further research to modify the integral equations in order to obtain a better result for added masses and their derivatives with respect to the separation distance in a region where the inviscid and irrotational theory itself is valid.

Motivated by the lack of studies on the oblique motion of solids, we have investigated the hydrodynamic interactions due to the off-center motion of a circular-cylinder pair and obtained analytical and numerical solutions. The motion of each body is assumed to be purely translational because at any time instant, the moment due to hydrodynamic interactions is zero. The kinetic energy of the fluid is first expressed in a polar coordinate system moving with the stream in terms of six added masses of the bodies due to their motions parallel and perpendicular to the line joining the centers. These added masses are in turn represented in a relative rectangular coordinate system as a function of the separation distance and of the angle between the uniform flow and the polar axis. By relating the absolute and relative frames of reference, the equations of motion, in Lagrangian form, are then integrated numerically for trajectories of the drifting body in space.

In Section 2, we are concerned with the Lagrange's equations of motion expressed in the relative and the absolute rectangular coordinates. The transformation of added masses from rectangular coordinates to polar ones is also considered in this section. Section 3 is mainly devoted to the exact, closed-form solutions of added masses and their derivatives for a pair of cylinders due

to centroidal and transversal motions respectively. In Section 4, we have studied the corresponding numerical solution based on the boundary integral method. The integral equations for the source distribution on each surface are carefully modified and the solutions are compared with the exact results. The trajectories of the moving body under various conditions are given and discussed in Section 5. Finally, conclusions are presented in Section 6.

II. EQUATIONS OF MOTION

Consider the motion of two circular cylinders in an unbounded fluid which moves with a uniform velocity U_o in the x direction at infinity. In an absolute frame of reference fixed in space, body 1 with center o_1 moves with velocities u and v in the x and y directions respectively, and body 2 with center o_2 is fixed in space. Relative to a moving frame of reference, in which the fluid is at rest at infinity, the center o_1, located at (x_1,y_1), moves with velocities U_1 and U_3 along the x and y directions respectively, while the center o_2, located at (x_2,o), moves with velocity U_2 along the x direction (see Fig.1a),

$$U_1 = u - U_o, \quad U_3 = v, \quad U_2 = -U_o. \tag{1}$$

The separation distance s between the centers is given by

$$s^2 = c^2 + h^2, \tag{2}$$

where $c = x_1 - x_2$ and $h = y_1$.

The fluid is assumed to be inviscid and incompressible and the flow irrotational. Hence, there exists a velocity potential ϕ which may be expressed as

$$\phi = U_1\phi_1 + U_2\phi_2 + U_3\phi_3, \tag{3}$$

where ϕ_1 is the unit velocity potential corresponding to $U_1=1$, $U_2 = 0$ and $U_3 = 0$, etc. The kinetic energy T of the fluid can then be expressed as

$$2T = A_{11}U_1^2+A_{22}U_2^2+A_{33}U_3^2+2A_{12}U_1U_2+2A_{13}U_1U_3+2A_{23}U_2U_3, \tag{4}$$

in which A_{ij}'s (i,j = 1,2,3) are added masses given by

$$A_{ij} = -\rho \int_{S_j} \phi_i \frac{\partial \phi_j}{\partial n_j} dS \qquad \text{(no sum on j)}, \tag{5}$$

$$A_{ij} = A_{ji} \quad . \tag{6}$$

ρ is the mass density of the fluid, $n_3 = n_1$, $S_3 = S_1$, n_j denotes distance along the outward normal to the jth body, and the integral extends over its surface S_j.

The motion of body 1, due to the hydrodynamic interaction, can be determined from the Lagrange's equations of motion,

$$M_1\frac{dU_1}{dt} = -\frac{d}{dt}\frac{\partial T}{\partial U_1} + \frac{\partial T}{\partial x_1} , \tag{7a}$$

$$M_1\frac{dU_3}{dt} = -\frac{d}{dt}\frac{\partial T}{\partial U_3} + \frac{\partial T}{\partial y_1} , \tag{7b}$$

where M_1 is the mass of body 1 and t is the time. The added mass A_{ij} depends on the separation distances c and h. From (2), we have

$$\frac{\partial T}{\partial x_1} = \frac{\partial T}{\partial c}, \quad \frac{\partial T}{\partial y_1} = \frac{\partial T}{\partial h}, \quad \frac{dc}{dt} = U_1-U_2, \quad \frac{dh}{dt} = U_3. \tag{8}$$

From equations (4),(7), and (8), we have

$$M_1\frac{dU_1}{dt} = -\frac{1}{2}\frac{\partial A_{11}}{\partial c}U_1^2 + (\frac{\partial A_{12}}{\partial c} + \frac{1}{2}\frac{\partial A_{22}}{\partial c})U_2^2 - (\frac{\partial A_{13}}{\partial h} - \frac{1}{2}\frac{\partial A_{33}}{\partial c})U_3^2 + \frac{\partial A_{11}}{\partial c}U_1U_2$$

$$-\frac{\partial A_{11}}{\partial h}U_1U_3 + (\frac{\partial A_{13}}{\partial c} - \frac{\partial A_{12}}{\partial h} + \frac{\partial A_{23}}{\partial c})U_2U_3 - (A_{11}\frac{dU_1}{dt} + A_{12}\frac{dU_2}{dt} + A_{13}\frac{dU_3}{dt}) , \tag{9a}$$

$$M_1\frac{dU_3}{dt} = (\frac{1}{2}\frac{\partial A_{11}}{\partial h} - \frac{\partial A_{13}}{\partial c})\,U_1^2 + (\frac{\partial A_{23}}{\partial c} + \frac{1}{2}\frac{\partial A_{22}}{\partial h})\,U_2^2 - \frac{1}{2}\frac{\partial A_{33}}{\partial h}U_3^2 - \frac{\partial A_{33}}{\partial c}U_1U_3$$

$$+(\frac{\partial A_{13}}{\partial c} - \frac{\partial A_{23}}{\partial c} + \frac{\partial A_{12}}{\partial h})\,U_1U_2 + \frac{\partial A_{33}}{\partial c}U_2U_3 - (A_{13}\frac{dU_1}{dt} + A_{23}\frac{dU_2}{dt} + A_{33}\frac{dU_3}{dt}) . \tag{9b}$$

From (1), we have

$$\frac{dU_2}{dt} = 0, \quad \frac{dU_1}{dt} = \frac{du}{dt}, \quad \frac{dU_3}{dt} = \frac{dv}{dt}, \quad U_3 = v . \tag{10}$$

By means of (1) and (10), we may simplify equations (9a,b) as

$$(M_1 + A_{11})\frac{du}{dt} + A_{13}\frac{dv}{dt} = -\frac{1}{2}\frac{\partial A_{11}}{\partial c}u^2 - (\frac{\partial A_{13}}{\partial h} - \frac{1}{2}\frac{\partial A_{33}}{\partial c})v^2 - \frac{\partial A_{11}}{\partial h}uv$$

$$+(\frac{1}{2}\frac{\partial A_{11}}{\partial c} + \frac{1}{2}\frac{\partial A_{22}}{\partial c} + \frac{\partial A_{12}}{\partial c})U_o^2 + (\frac{\partial A_{11}}{\partial h} + \frac{\partial A_{12}}{\partial h} - \frac{\partial A_{13}}{\partial c} - \frac{\partial A_{23}}{\partial c})U_o v, \tag{11a}$$

$$(M_1 + A_{33})\frac{dv}{dt} + A_{13}\frac{du}{dt} = (\frac{1}{2}\frac{\partial A_{11}}{\partial h} - \frac{\partial A_{13}}{\partial c})\,u^2 - \frac{1}{2}\frac{\partial A_{33}}{\partial h}v^2 - \frac{\partial A_{33}}{\partial c}uv$$

$$+(\frac{1}{2}\frac{\partial A_{11}}{\partial h} + \frac{1}{2}\frac{\partial A_{22}}{\partial h} + \frac{\partial A_{12}}{\partial h})\,U_o^2 - (\frac{\partial A_{11}}{\partial h} + \frac{\partial A_{12}}{\partial h} - \frac{\partial A_{13}}{\partial c} - \frac{\partial A_{23}}{\partial c})U_o u . \tag{11b}$$

The added masses in equations (9a,b) and (11a,b) are functions of c and h and evaluated in the rectangular coordinates.

For a pair of circular cylinders, we may represent the motion of body 1 in a polar coordinate system centered at $(x_2, 0)$,

$$x_1 = x_2 + s\cos\gamma,$$
$$y_1 = s\sin\gamma, \tag{12}$$

and decompose each added mass into a part depending on the separation distance s and another on the angle γ between the centerline o_1o_2 and the x axis (Fig.1b). Let A'_{ij} (i,j = 1,2,3,4) be the added masses evaluated in the polar coordinates corresponding to the unit velocities U_i', where U_1' and U_2' are velocities of body 1 and body 2 respectively along the direction of the centerline o_1o_2, U_3' and U_4' are the corresponding velocity components perpendicular to o_1o_2 (Fig.1b). Since body 1 and body 2 are symmetric with respect to the centerline o_1o_2, a sign change in U'_3 should not change the fluid kinetic energy in terms of A'_{ij}. Therefore $A'_{13}=0$. Similarly, $A'_{14} = A'_{23} = A'_{24} =0$. Based on the invariance of the kinetic energy to the coordinate transformation, we obtain the relation

$$A_{11} = A'_{11}\cos^2\gamma + A'_{33}\sin^2\gamma, \qquad A_{33} = A'_{11}\sin^2\gamma + A'_{33}\cos^2\gamma,$$

$$A_{22} = A'_{22}\cos^2\gamma + A'_{44}\sin^2\gamma, \qquad A_{12} = A'_{12}\cos^2\gamma + A'_{34}\sin^2\gamma,$$

$$A_{13} = (A'_{11} - A'_{33})\sin\gamma\cos\gamma, \qquad A_{23} = (A'_{12} - A'_{34})\sin\gamma\cos\gamma. \qquad (13)$$

The derivatives of A_{ij} with respect to c and h are then expressed as functions of s and γ,

$$\frac{\partial A_{11}}{\partial c} = [\frac{\partial A'_{11}}{\partial s}\cos^2\gamma + \frac{\partial A'_{33}}{\partial s}\sin^2\gamma]\cos\gamma + 2(-A'_{11} + A'_{33})\cos\gamma\sin\gamma(-\frac{\sin\gamma}{s}),$$

$$\frac{\partial A_{11}}{\partial h} = [\frac{\partial A'_{11}}{\partial s}\cos^2\gamma + \frac{\partial A'_{33}}{\partial s}\sin^2\gamma]\sin\gamma + 2(-A'_{11} + A'_{33})\cos\gamma\sin\gamma(\frac{\cos\gamma}{s}), \quad \text{etc.} \qquad (14)$$

Relying on the foregoing transformation, we can consider the added masses due to centroidal and transversal motions, separately, at any time instant.

III. ADDED MASSES AND THEIR DERIVATIVES

The added masses of two bodies moving through an inviscid and incompressible fluid can be determined in terms of hydrodynamic singularities within each body, by means of a

generalization of Taylor's added-mass theorem[9]. For a pair of three-dimensional solids moving in any manner except pure rotations, the generalized Taylor's added-mass formula is given as

$$A_{i\alpha j\beta} + \delta_{\alpha\beta}\delta_{ij} M'_\beta = 4\pi\rho \left[\int_{V_\beta} -x_j \lambda_{i\alpha\beta} dV + \sum (m_{i\alpha\beta} x^o_j + \mu_{i\alpha j\beta}) \right]$$

(no sum on β), (15)

where $A_{i\alpha j\beta}$ are added masses[7] of body β along the j-th direction due to the unit motion of body α in the i-th direction, M'_β is the mass of the fluid displaced by body β, $\lambda_{i\alpha\beta}$ and $m_{i\alpha\beta}$ are the volume-distributed source density and the isolated source strength, respectively, inside body β due to the i-th velocity component of body α, $\mu_{i\alpha j\beta}$ is the strength of an isolated dipole in the j-th direction inside body β associated with the i-th velocity component of body α, x_j and x^o_j are the j-th local coordinates of $\lambda_{i\alpha\beta}$ and $m_{i\alpha\beta}$ respectively with respect to body β, the integration is over the volume of body β, V_β, and the summation is over all isolated singularities inside V_β. The factor 4 in equation (15) should be changed to 2 for a pair of two-dimensional bodies. The distributed doublets do not appear explicitly in (15) because, by integration by parts, they are equivalent to a distribution of sources in V_β plus a surface distribution of sources on the boundary[10]. For the present two-dimensional problem, (15) may be simplified as

$$A_{ij} + \delta_{ij} M'_j = 2\pi\rho \left[\int_{V_j} -x_j \lambda_i dV + \sum (m_i x^o_j + \mu_{ij}) \right]$$

(no sum on j), (16)

where the corresponding notations are defined in a similar manner to the foregoing ones.

When two circular cylinders move along the centerline o_1o_2, with velocities U'_1 and U'_2 respectively, the method of successive images (Hicks[5], Müller[8]) can be applied to obtain added masses. This method, based on Taylor's added-mass formula (16) and the circle theorem, produces simple expressions for added masses in terms of the strengths of isolated doublets inside circles which represent an equivalent velocity potential due to the motion of solids.

Consider first the system of hydrodynamic singularities corresponding to the unit motion of circle 1 along the centerline o_1o_2, $U'_1 = 1$, $U'_2 = U'_3 = U'_4 = 0$ (Fig.1b). If circle 2 were absent, the velocity potential could be represented by a doublet of strength $\mu_o = a^2$ located at o_1 in the direction of U'_1 (Fig.2). However, the presence of circle 2 violates the boundary condition on surface 2 and needs an image doublet of strength $\mu_1 = - a^2b^2/s^2$ at the inverse point P_1 inside circle 2 to satisfy the boundary condition on circle 2, where the minus sign for μ_1 indicates that the doublet is in the opposite direction of U'_1 and the point P_1 is on the centerline o_1o_2 with $P_1o_2 = b^2/s$ (Fig.2). The presence of this image doublet violates the boundary condition on surface 1 and requires another isolated image doublet inside circle 1 and so on. The general expression for the strengths and positions of the 2n-th (in circle 1) and the (2n+1)-th (in circle 2) doublets is given by the iterative formula (Rouse et al.[11])

$$\mu_o = a^2, \quad \lambda_o = s,$$

$$\mu_{2n+1} = - \mu_{2n} \left(\frac{b^2}{\lambda_{2n}{}^2} \right),$$

$$\lambda_{2n+1} = s - \frac{b^2}{\lambda_{2n}},$$

$$\mu_{2n+2} = - \mu_{2n+1} \left(\frac{a^2}{\lambda_{2n+1}{}^2} \right),$$

$$\lambda_{2n+2} = s - \frac{a^2}{\lambda_{2n+1}}, \qquad (n=0,1,2,...), \tag{17}$$

where λ_{2n} denotes the distance from o_2 to the n-th inverse point in circle 1 and λ_{2n+1} that from o_1 to the (n+1)-th inverse point in circle 2, all inverse points lie on the centerline o_1o_2. As n tends to infinity, the system of doublets generates the same velocity potential exterior to the circles as that due to the unit motion of circle 1 along o_1o_2.

To find the closed-form expression of added masses from the iterative formula (17), it is necessary to represent the doublet strength at the n-th iteration in terms of radii a, b, and the separation distance s. A series expansion of added masses of two spheres due to their centroidal motion was derived by Hicks[5] and Herman[12] by means of the method of continued fraction. Their result was also generalized, with slight modifications, to the case of two or multiple cylinders by Müller[8] and Yamamoto[3]. However, an alternative expansion is used in the present study so that we may find the derivatives of added masses with respect to s easily.

Equation (17) can be reduced to

$$\mu_{2n} = a^2 \frac{(a\ b)^{2n}}{(\lambda_o\lambda_1\lambda_2...\lambda_{2n-1})^2}\ , \tag{18a}$$

$$\mu_{2n+1} = -\frac{(a\ b)^{2n+2}}{(\lambda_o\lambda_1\lambda_2...\lambda_{2n})^2} \quad (n = 0,\ 1,\ 2,\ ...\ )\ . \tag{18b}$$

For every n, the location of the inverse point satisfies the relations

$$\lambda_{2n}\lambda_{2n+1} = s\lambda_{2n} - b^2,\quad \lambda_{2n+1}\lambda_{2n+2} = s\lambda_{2n+1} - a^2\ . \tag{19}$$

After some manipulation, it can be found that

$$\lambda_{2n-1}\lambda_{2n-2}....\lambda_o = \frac{a^2(r_1{}^n - r_2{}^n) + (r_1{}^{n+1} - r_2{}^{n+1})}{r_1 - r_2}, \tag{20a}$$

and

$$\lambda_{2n}\lambda_{2n-1}....\lambda_1 = \frac{r_1{}^{n+1} - r_2{}^{n+1}}{r_1 - r_2}, \tag{20b}$$

where

$$r_{1,2} = \frac{1}{2}\left[\ (s^2 - a^2 - b^2) \pm \sqrt{\ (s^2 - a^2 - b^2)^2 - 4\ a^2b^2\ }\ \right]. \tag{21}$$

The n-th image-doublet strength inside circle 1 is then

$$\mu_{2n} = a^2 \frac{(a\ b)^{2n}}{[a^2(r_1^{n-1}+r_1^{n-2}r_2+\ldots+r_2^{n-1})+(r_1^{n}+r_1^{n-1}r_2+\ldots+r_2^{n})]^2} \tag{22a}$$

and that inside circle 2 is

$$\mu_{2n+1} = -\frac{(a\ b)^{2n+2}}{s^2(r_1^{n}+r_1^{n-1}r_2+\ldots+r_2^{n})^2} \ . \tag{22b}$$

For a fixed n, the limits of sequences $\{\mu_{2n}\}$, $\{\mu_{2n+1}\}$ as s approaches (a+b) are derived as

$$\lim_{s\to(a+b)} \mu_{2n} = \frac{a^2\ b^2}{(n(a\ +\ b)\ +\ b)^2}\ , \tag{23a}$$

$$\lim_{s\to(a+b)} \mu_{2n+1} = -\frac{a^2\ b^2}{(a+b)^2(n+1)^2}\ . \tag{23b}$$

$\{\mu_{2n}\}$ and $\{\mu_{2n+1}\}$ are uniformly convergent for any values of s in the region $[a+b,\infty)$ since in the limit, $s\to(a+b)$, (23a,b) decay by the rate of $1/n^2$ and for $s > (a+b)$,

$$\frac{\mu_{2n+2}}{\mu_{2n}} = \left(\frac{ba}{\lambda_{2n}\lambda_{2n+1}}\right)^2 < 1 \qquad \text{and} \qquad \frac{\mu_{2n+1}}{\mu_{2n-1}} = \left(\frac{ba}{\lambda_{2n-1}\lambda_{2n}}\right)^2 < 1.$$

Substitution of μ_{2n} and μ_{2n+1} into Taylor's added-mass formula (16) yields the expression of added masses due to the centroidal motion of two circles in the relative polar coordinates

$$A'_{11} = 2\pi\rho\ [\ \sum_{n=0}^{\infty} \mu_{2n} - \frac{a^2}{2}\ ]\ ,$$

$$A'_{12} = 2\pi\rho\ \sum_{n=0}^{\infty} \mu_{2n+1}\ ,$$

$$A'_{22} = 2\pi\rho \left[\sum_{n=0}^{\infty} \mu^*_{2n} - \frac{b^2}{2} \right],$$

$$A'_{21} = A'_{12}, \tag{24}$$

where ρ is the density of the fluid, μ^*_{2n} denotes the doublet strength inside circle 2 due to the unit motion of itself along the centerline o_1o_2, $U'_2=1$, $U'_1=U'_3=U'_4=0$, and is obtained directly by interchanging a and b in equation (17). The limiting values of added masses, as s approaches (a + b), are obtained from expressions (23a,b) and (24)

$$\lim_{s\to(a+b)} A'_{11} = 2\,\pi\,\rho \left[\frac{a^2\,b^2}{(a+b)^2} \sum_{n=0}^{\infty} \frac{1}{\left(n + \frac{b}{a+b}\right)^2} - \frac{a^2}{2} \right], \tag{25a}$$

$$\lim_{s\to(a+b)} A'_{12} = -2\,\pi\,\rho\,\frac{a^2\,b^2}{(a+b)^2}\,\zeta(2) = -3.28968\,\pi\,\rho\,\frac{a^2\,b^2}{(a+b)^2}, \tag{25b}$$

where $\zeta(2)$ is the zeta function. From (22a,b) and (24), we note that, as s increases from (a+b) to infinity, the added mass A'_{11} decreases monotonically from its limiting value given in (25a) to a constant $\pi\rho a^2$ and the interaction added mass A'_{12} increases monotonically from the value given in (25b) to zero.

To evaluate the derivatives of added masses directly from equation (24) by differentiating each term of sequences $\{\mu_{2n}\}$ and $\{\mu_{2n+1}\}$ with respect to s, we need to prove that in a certain region of s, the sequences $\{d\mu_{2n}/ds\}$ and $\{d\mu_{2n+1}/ds\}$ are uniformly convergent. By taking the derivatives of μ_{2n} and μ_{2n+1} directly from (18), we have

$$\frac{d\mu_{2n}}{ds} = -2\,\frac{a^2\,a^{2n}\,b^{2n}}{(\lambda_{2n-1}\lambda_{2n-2}\ldots\lambda_o)^3}\,\frac{d}{ds}\,(\lambda_{2n-1}\lambda_{2n-2}\ldots\lambda_o), \tag{26a}$$

and

$$\frac{d\mu_{2n+1}}{ds} = \frac{2\,(a\,b)^{2n+2}}{s^3(\lambda_{2n}\lambda_{2n-1}....\lambda_1)^2}\left[1+\frac{s}{\lambda_{2n}\lambda_{2n-1}....\lambda_1}\,\frac{d}{ds}\,(\lambda_{2n}\lambda_{2n-1}....\lambda_1)\right]\ . \qquad (26b)$$

Let Π_o be the product $\lambda_{2n-1}\lambda_{2n-2}....\lambda_o$. Since, from (21),

$$\frac{dr_1}{ds} = \frac{2s\,r_1}{r_1-r_2},\quad \frac{dr_2}{ds} = -\frac{2s\,r_2}{r_1-r_2}, \text{ and } r_1r_2=(ab)^2, \qquad (27)$$

the differential part of (26a) becomes

$$\frac{d\Pi_o}{ds} = \frac{\partial\Pi_o}{\partial r_1}\frac{dr_1}{ds} + \frac{\partial\Pi_o}{\partial r_2}\frac{dr_2}{ds}$$

$$=\frac{2s}{(r_1-r_2)^3}\{-(ab)^2a^2(n+1)(r_1^{n-1}-r_2^{n-1})+a^2(n-1)(r_1^{n+1}-r_2^{n+1})+n(r_1^{n+2}-r_2^{n+2})-(n+2)(ab)^2(r_1^{n}-r_2^{n})\}. \qquad (28)$$

The limiting value of (26a) for fixed $s > (a+b)$ is

$$\lim_{n\to\infty}\frac{d\mu_{2n}}{ds} = -\lim_{n\to\infty}\frac{4\,a^2(ab)^{2n}\,s\,n}{\Pi_o^2(r_1-r_2)} = 0. \qquad (29)$$

Based on the ratio test,

$$\lim_{n\to\infty}\frac{d\mu_{2n+2}/ds}{d\mu_{2n}/ds} = \frac{(ab)^2}{(\lambda_{2n}\lambda_{2n+1})^2} < 1,$$

we conclude that the sequence $\{d\mu_{2n}/ds\}$ is uniformly convergent in the region $(a+b, \infty)$. Similarly, we can prove that the sequence $\{d\mu_{2n+1}/ds\}$ is also uniformly convergent in the same region. Thus, the derivatives of added masses (24) with respect to s are equal to the summations of derivatives of the corresponding doublet strengths for $(a+b) < s < \infty$.

From (17) and (24), we have

$$\frac{d\mu_o}{ds} = 0,\quad \frac{d\lambda_o}{ds} = 1,$$

$$\frac{d\mu_{2n+1}}{ds} = -\frac{d\mu_{2n}}{ds}\left(\frac{b^2}{\lambda_{2n}^2}\right) + 2\mu_{2n}\left(\frac{b^2}{\lambda_{2n}^3}\right)\left(\frac{d\lambda_{2n}}{ds}\right),$$

$$\frac{d\lambda_{2n+1}}{ds} = 1 + \left(\frac{b^2}{\lambda_{2n}^2}\right)\left(\frac{d\lambda_{2n}}{ds}\right),$$

$$\frac{d\mu_{2n+2}}{ds} = -\frac{d\mu_{2n+1}}{ds}\left(\frac{a^2}{\lambda_{2n+1}^2}\right) + 2\mu_{2n+1}\left(\frac{a^2}{\lambda_{2n+1}^3}\right)\left(\frac{d\lambda_{2n+1}}{ds}\right),$$

$$\frac{d\lambda_{2n+2}}{ds} = 1 + \left(\frac{a^2}{\lambda_{2n+1}^2}\right)\left(\frac{d\lambda_{2n+1}}{ds}\right), \tag{30}$$

and

$$\frac{dA'_{11}}{ds} = 2\pi\rho \sum_{n=0}^{\infty} \frac{d\mu_{2n}}{ds}, \qquad \frac{dA'_{12}}{ds} = 2\pi\rho \sum_{n=0}^{\infty} \frac{d\mu_{2n+1}}{ds},$$

$$\frac{dA'_{22}}{ds} = 2\pi\rho \sum_{n=0}^{\infty} \frac{d\mu^*_{2n+1}}{ds}, \qquad \frac{dA'_{21}}{ds} = \frac{dA'_{12}}{ds}. \tag{31}$$

The region of convergence for derivatives of added masses in (31) is open on the left since the limiting value of (29) is not zero as s approaches (a+b).

The above analysis for added masses and their derivatives indicates that, as the separation distance s tends to (a+b), the kinetic energy of the fluid due to the motion of solids is finite but the hydrodynamic interaction forces, which are functions of the derivatives of added masses with respect to s, approach infinity.

When two circles make transversal motions perpendicular to the centerline o_1o_2, the strengths and locations of doublets in each circle can be determined in the same way as that used for the centroidal motion. Thus, we have

$$A'_{11} = A'_{33}, \quad A'_{22} = A'_{44}, \quad A'_{12} = -A'_{34}. \tag{32}$$

Since the summations of doublet strengths and their derivatives with respect to s, given by iterative formulas (17) and (30), are convergent to the corresponding solutions of added masses and their derivatives, we can calculate them numerically based on these iterative formulas and obtain the results as accurate as we want by increasing the index n to a sufficiently large number. Practically, if s is larger than 1.5(a+b), an accuracy of five significant figures can be achieved within a few iterations and for $(a+b) < s < 1.01\ (a+b)$, the same accuracy may need several hundred iterations.

IV. NUMERICAL SOLUTION OF ADDED MASSES AND THEIR DERIVATIVES

The application of the afore-mentioned analysis is limited by the body geometry and flow conditions since, in general, the velocity potential cannot be expressed in terms of isolated interior singularities. For bodies of various geometries, however, we may have to evaluate added masses and their derivatives numerically in terms of certain distributed singularities either inside bodies or on the body surfaces. Landweber & Chwang[7] has developed a boundary-integral method for two-body interaction problems based on the generalized Taylor's formula and the fundamental relation between the velocity potential and normal velocities on solid boundaries. The accuracy of their method depends on the simultaneous solutions of a set of Fredholm integral equations of the second kind. Due to the singular behavior of the kernels in these equations, some numerical inaccuracy in the solutions may be significant when two bodies are very close to each other. In order to investigate the reliability and to improve the accuracy of numerical results, we shall consider a pair of circles again and compare the numerical results with exact solutions.

From the work of Landweber & Chwang[7], added masses due to the general translational motion of a pair of two-dimensional bodies are given by

$$A_{i\alpha j\beta} = 2\pi\rho \int x_j \sigma_{i\alpha\beta} dS_\beta - M'_\beta \delta_{ij}\delta_{\alpha\beta} \quad \text{(no sum on } \beta\text{)}, \tag{33}$$

where ρ is the density of the fluid, M'_β (β=1,2) is the mass of the fluid displaced by body β, $\sigma_{i\alpha\beta}$ denotes the surface source distribution on body β due to the i-th unit velocity component of body α, and x_j is the coordinate of the surface source on body β. For the relative motion of two circles concerned in the present study, the unknown surface source distributions satisfy a set of integral equations

$$\pi E(P) + \int F(Q') \frac{\cos \psi_{12}}{R_{21}} dS_2 = U'_1 \frac{\partial x}{\partial n_1} + U'_3 \frac{\partial y}{\partial n_1}, \tag{34a}$$

$$\pi F(Q) + \int E(P') \frac{\cos \psi_{21}}{R_{12}} dS_1 = U'_2 \frac{\partial x}{\partial n_2} + U'_4 \frac{\partial y}{\partial n_2}, \tag{34b}$$

where E(P) denotes the unknown source strength at point P on circle 1, F(Q) denotes that at point Q on circle 2, R_{ij} is the distance between the source point on body i and the field point on the surface of body j, n_i indicates the outward normal direction at the field point on the surface of body i, and ψ_{ij} is the angle between n_i and R_{ji} (Fig.3a). In the derivation of equation(34a,b), integrals involving the kernel $(\cos \psi_{11})/R_{11}$ or $(\cos \psi_{22})/R_{22}$ reduce to zero for circles, since they are constant on circles 1 and 2 and the integrals of E and F over closed bodies vanish identically.

To obtain the added masses, we first set $U'_1 = 1$, $U'_2 = U'_3 = U'_4 = 0$. The solution of (34) for this condition yields the source distributions for evaluating A'_{11} and A'_{12},

$$A'_{11} = 2\pi\rho a^2 \int_0^{2\pi} E(\alpha) \cos\alpha \, d\alpha - \rho\pi a^2, \tag{35a}$$

$$A'_{12} = 2\pi\rho b^2 \int_0^{2\pi} F(\theta) \cos\theta \, d\theta . \tag{35b}$$

Similarly, A'_{22} is obtained by using the source density F determined from the condition that $U'_2 = 1$ and $U'_1 = U'_3 = U'_4 = 0$,

$$A'_{22} = 2\pi\rho b^2 \int_0^{2\pi} F(\theta) \cos\theta \, d\theta - \rho\pi b^2. \tag{35c}$$

From (32) and the symmetry argument leading to (13), we have

$$A'_{13} = A'_{14} = A'_{23} = A'_{24} = 0, \tag{35d}$$

$$A'_{11} = A'_{33}, \quad A'_{22} = A'_{44}, \quad A'_{12} = - A'_{34}. \tag{35e}$$

The dimensionless added-mass coefficients may be defined as

$$k_{ij} = A'_{ij} / M'_1. \tag{36}$$

All integrations in equations (34a,b) are regular for $s > (a+b)$. However, by comparing the analytical solution of added masses from equations (17) and (24) with the numerical result from integral equations (34) and (35) (Table 1, columns with superscripts "e" and "a"), we recognize that a considerable deviation in the numerical result takes place when $s = a+b+\delta$, $\delta << 1$. The numerical error comes mainly from two sources, one due to the ill-conditioned kernels which have a large and steep peak value of order $o(1/\delta)$ in the region around $\alpha=\pi$ and $\theta=0$ (Fig.3a), and another due to the discretization of the integral equations into a set of linear algebraic equations. In order to remove the peaks, we subtract a function, which has the same peak value and similar behavior around $\alpha=\pi$ and $\theta=0$, from the integral and then add the exact integration of the function back to the equation. Thus, equation(34a,b) is modified to

$$\pi E(\alpha) + b \int_0^{2\pi} [F(\theta') \frac{\cos\psi_{12}}{R_{21}}(\alpha,\theta') - F(0)\, g_1(\alpha,\theta')] d\theta' + b \int_0^{2\pi} F(0)\, g_1(\alpha,\theta') d\theta'$$

$$= U'_1 \cos\alpha + U'_3 \sin\alpha, \tag{37a}$$

$$\pi F(\theta) + a \int_0^{2\pi} [E(\alpha') \frac{\cos\psi_{21}}{R_{12}}(\alpha',\theta) - E(\pi)\, g_2(\alpha',\theta)] d\alpha' + a \int_0^{2\pi} E(\pi)\, g_2(\alpha',\theta) d\alpha'$$

$$= U'_2\cos\theta + U'_4\sin\theta, \tag{37b}$$

where

$$\frac{\cos\psi_{12}}{R_{21}} = \frac{a - b\cos(\theta' - \alpha) + s\cos\alpha}{(s - b\cos\theta' + a\cos\alpha)^2 + (b\sin\theta' - a\sin\alpha)^2}, \tag{38a}$$

$$\frac{\cos\psi_{21}}{R_{12}} = \frac{b - a\cos(\theta - \alpha') - s\cos\theta}{(s - b\cos\theta + a\cos\alpha')^2 + (b\sin\theta - a\sin\alpha')^2}. \tag{38b}$$

For simple kernels like (38a,b), we may let g_1 and g_2 be $(\cos\psi_{12})/R_{21}$ and $(\cos\psi_{21})/R_{12}$ respectively. Then integrations of g_1 and g_2 on circles 2 and 1, respectively, give (Fig.3)

$$b\int_0^{2\pi} g_1(\alpha,\theta')d\theta' = \frac{2\pi b}{d}\cos(\alpha - \beta), \tag{39a}$$

$$a\int_0^{2\pi} g_2(\alpha',\theta)d\alpha' = -\frac{2\pi a}{d^*}\cos(\theta + \beta^*), \tag{39b}$$

where

$$d^2 = s^2 + a^2 + 2as\cos\alpha, \qquad d^{*2} = s^2 + b^2 - 2sb\cos\theta, \tag{40}$$

and

$$\beta = \pm\cos^{-1}\left(\frac{s^2 + d^2 - a^2}{2ds}\right), \qquad \beta^* = \pm\cos^{-1}\left(\frac{s^2 + d^{*2} - b^2}{2d^*s}\right). \tag{41}$$

The positive branches of β and β^* correspond to $0 < \alpha < \pi$ and $0 < \theta < \pi$ respectively, and the negative ones to $\pi < \alpha < 2\pi$ and $\pi < \theta < 2\pi$. Numerical results of k_{11} and k_{12}, defined by equation (36), based on the modification are listed in Table 1. From columns with superscript "c" in Table 1, we note immediately the significant improvement based on equation (37).

Although the integrands in equation (37a,b) vanish at $\theta=0$ and $\alpha=\pi$, they have not been quite smoothed in that neighborhood. In this peak region, the difference of source strengths $F(\theta')-F(0)$ or $E(\alpha')-E(\pi)$ is not large, but its product with the ill-conditioned kernel can become

very large, especially for the centroidal motion, such that it affects the evaluation of the integrals significantly. The accuracy may be further improved by choosing an appropriate quadrature formula. It has been proved by Atkinson[13] that if the integrand is a periodic function and the domain of integration is evenly discretized, the trapezoidal rule provides the best numerical estimation of the integral. However, it is clear that we should put more points in the peak region and less points in the region where the integrand slopes gently. In the present calculation, we subdivide the region of integration into two parts, one contains the sharp peak and the other covers the rest(Fig.4), and in each subdivision, evaluate integrals in Eq. (37a,b) by the Gaussian quadrature formula. In order to compare numerical results of the integration in the peak region, obtained by the Gaussian quadrature formula and by the trapezoidal rule, with the exact solution, we examine the integral

$$I = \int_0^{2\pi} \frac{\cos \psi_{12}}{R_{21}}(\alpha,\theta') \, d\theta', \tag{42}$$

where $(\cos \psi_{12})/R_{21}$ is given by (38a) and α is the angle between o_1o_2 and o_1P(Fig.3b). At $s = a+b+\delta$ and $a/b = 1.0$, the integrand in (42) has a peak of the order of $o(1/\delta)$ around $\alpha = \pi$ and $\theta' = 0$. The results are given in Fig. 5. From this figure, we observe that the deviation of the numerical results obtained by the Gaussian quadrature formula from the exact solution is much smaller than that by the trapezoidal rule. For $a/b = 1$ and various values of s, the numerical results of added-mass coefficients, k_{11} and k_{12}, obtained by the trapezoidal rule with 80 points and by the Gaussian quadrature formula with 60 points along each circle, are listed in Table 1(columns "b" and "c"). The latter has only less than 1% error at s=2.01, while the former does not converge at s = 2.01 and has 1.4% error for k_{12} at s=2.04. The size of the subdivision on each circle depends surely on the separation distance s, since the peak becomes sharper as s is closer to (a+b). In the

present calculation, the divisions are roughly estimated and their sizes, measured by the angle ω for a=b, are listed in Table 1.

In order to find derivatives of added masses with respect to the separation distance s in terms of the boundary integrals, it is necessary to evaluate the derivative of the surface source distribution with respect to s. For two circles, the derivatives are given implicitly by a pair of Fredholm integral equations of the second kind,

$$\pi E_s(\alpha)+b\int_0^{2\pi}[F_s(\theta')-F_s(0)]\frac{\cos\psi_{12}}{R_{21}}(\alpha,\theta')\,d\theta'+$$

$$b\int_0^{2\pi}[F(\theta')-F(0)]\,\frac{d}{ds}\left(\frac{\cos\psi_{12}}{R_{21}}(\alpha,\theta')\right)d\theta' = -P(\alpha), \tag{43a}$$

$$\pi F_s(\theta)+a\int_0^{2\pi}[E_s(\alpha')-E_s(\pi)]\frac{\cos\psi_{21}}{R_{12}}(\alpha',\theta)\,d\alpha'+$$

$$a\int_0^{2\pi}[E(\alpha')-E(\pi)]\,\frac{d}{ds}\left(\frac{\cos\psi_{21}}{R_{12}}(\alpha',\theta)\right)d\alpha' = -Q(\theta), \tag{43b}$$

where $E_s(\alpha)$ and $F_s(\theta)$ stand for $dE(\alpha)/ds$ and $dF(\theta)/ds$ on circles 1 and 2 respectively, and

$$P(\alpha) = b\int_0^{2\pi}\left[F_s(0)\frac{\cos\psi_{12}}{R_{21}}(\alpha,\theta')+F(0)\frac{d}{ds}\left(\frac{\cos\psi_{12}}{R_{21}}(\alpha,\theta')\right)\right]d\theta'$$

$$= \frac{2\pi b}{d}\left\{F_s(0)\cos(\alpha-\beta)-\frac{F(0)}{d^2}[a\cos\beta+s\cos(\alpha-\beta)]\right\}, \tag{44a}$$

$$Q(\theta) = a\int_0^{2\pi}\left[E_s(\pi)\frac{\cos\psi_{21}}{R_{12}}(\alpha',\theta)+E(\pi)\frac{d}{ds}\left(\frac{\cos\psi_{21}}{R_{12}}(\alpha',\theta)\right)\right]d\alpha'$$

$$= -\frac{2\pi a}{d^*}\left\{E_s(\pi)\cos(\theta+\beta^*)+\frac{E(\pi)}{d^{*2}}[b\cos\beta^*-s\cos(\theta+\beta^*)]\right\}. \tag{44b}$$

Following the procedure in solving (37a,b), we subdivide the region of integrations into two parts, and in each subdivision, evaluate integrals in (44a,b) by the Gaussian quadrature formula. The set of integral equations in (44a,b) is then solved by the Gauss-Seidel iterative method. After the determination of functions $E_s(\alpha)$ and $F_s(\theta)$, the derivatives of added masses can be obtained by simple integrations. For example, from (35a) and (35b), we have

$$\frac{dA'_{11}}{ds} = 2\pi\rho a^2 \int_0^{2\pi} E_s(\alpha)\cos\alpha \, d\alpha ,$$

$$\frac{dA'_{12}}{ds} = 2\pi\rho b^2 \int_0^{2\pi} F_s(\theta)\cos\theta \, d\theta . \qquad (45)$$

An accurate solution of (43a,b) is more difficult to obtain than that of (37a,b) when two bodies are close to each other, since the kernels $d(\cos\psi_{12}/R_{21})/ds$ and $d(\cos\psi_{21}/R_{12})/ds$ in (44a,b) have peaks of the order of $o(1/\delta^2)$ in the region around $\alpha=\pi$ and $\theta=0$. To solve this problem, we simply add more points in the peak region when s is close to (a+b). For a/b=1.0, all integrals in equations (44a,b) are evaluated by the 160-point Gaussian quadrature for $2.0 < s < 2.1$ and by the 60-point Gaussian quadrature for $s > 2.1$. The numerical values of the derivatives of added-mass coefficients are compared with the exact ones in Table 2. At s = 2.01, the error for the derivative of k_{11} with respect to s is 2.6% and that for dk_{12}/ds is 2.5%. For $s \geq 2.02$, however, the results of (45) based on solutions of (43a,b) agree with the exact values up to 5 significant figures. Therefore, they may be regarded as exact for all practical purposes.

V. NUMERICAL RESULTS ON TRAJECTORIES

For a pair of circular cylinders, the added masses and their derivatives with respect to s have been evaluated exactly by the method of successive images and approximately by the boundary integral method. By (13) and (14), the results obtained in the relative polar coordinates can be transformed into the Cartesian coordinates in which the motions of bodies are described.

With $A_{13} = 0$ and $A_{11} = A_{33}$, the Lagrange's equations of motion(11a,b) are decoupled and simplified. The instantaneous velocity components u and v of circle 1, which are functions of added masses and their derivatives with respect to c and h(Fig.1), are given by the first integration of (11a,b) with respect to t. The trajectories of the moving circle around the fixed one, are then integrated from u and v. In the calculation, the origin of the absolute coordinate system is located at the center of the fixed body. We assume that the uniform flow conveying the drifting body is U_o= 1.0 along the x direction at infinity. When two circles are far away from each other, we may specify the initial condition used in the solution as $u_o = 1.0$, $v_o = 0.0$ for $s_o/(a+b) > 10$. Numerically, we discretize the time t into a number of intervals, δt_i (i=0,1,2, ...), and assume that within each time interval, velocities u and v are constants which are the same as those at the beginning of the interval. The lengths of δt are taken as $\delta t_i = 0.1$ when $x < -3$ and $\delta t_i = 0.01$ when x is larger than -3.

The computation is started at the initial position (x_o, y_o), where $x_o = -20$ for $b = 1$, $a \leq 1$ and y_o varies. At the beginning of each interval δt_i, u_i and v_i are obtained by the fourth- order Runge-Kutta integration of (11a,b) in terms of velocities in the previous interval, u_{i-1} and v_{i-1}, the added masses, and their derivatives. By the end of this interval, the new position of the drifting circle is given by

$$x_i = x_{i-1} + u_i \delta t_i \quad \text{and} \quad y_i = y_{i-1} + v_i \delta t_i \, .$$

This process is repeated until the separation distance s is equal to or less than (a + b), at which impact between two bodies takes place. The radii a and b are normalized by that of the fixed cylinder. Various ratios of a/b, depending on different physical problems, are considered in the calculation.

We first consider a circular cylinder of ice with radius a = 0.1 and density ρ=0.91, moving around a fixed cylinder of radius b=1.0. At y_o=0.1, 0.3, etc., the trajectories of the ice particle are plotted in Figures 6a to 6e for different density ratios of the body to the fluid medium. Fig.6a

corresponds to the case of an ice particle moving in fresh water and Fig.6e shows the same ice particle in an air flow. The ratios 2.0, 5.0 and 10.0 correspond to various fluid media and illustrate the change of trajectories with respect to the density ratio. We note from these figures that the lower the density ratio is, the larger the curvature of trajectories would be. In the case of an ice particle carried by an air flow, its trajectories are almost straight lines which differ from the streamlines greatly. It means that in a fluid of high density, the hydrodynamic interaction due to the presence of a second body has a large effect on the body's motion.

In some physical problems, for example, in the ice coating process, it is important to determine whether or not a drifting body, conveyed by a current, can impact with a fixed body. This physical property can be expressed by a "collection coefficient" E which is defined as the ratio of a critical initial position y^*_o, below which the drifting body will impact with the fixed body, to the radius of the fixed body. y^*_o is surely depending on the ratios of a/b and ρ_a/ρ. In this type of problems, the size of the moving body is much smaller than that of the fixed one. Fig.7 shows the result of the collection coefficient for a pair of cylinders, $0.01 \leq a/b \leq 1$, in fluids of different densities. Moving bodies of very small size are not considered since the Reynold's number becomes quite small such that the inviscid-fluid theory is not applicable.

Regarding to a floating body in sea water, we can consider the interaction problem between an ice floe, idealized as a cylinder, and a fixed cylindrical offshore-structure. Fig.8 shows the trajectories of a circular cylinder in sea water. Here the density ratio ρ_a/ρ is fixed at 0.89, which corresponds to a floating ice in sea water. The radius ratio a/b is 0.5 in Fig.8a and 1.0 in Fig.8b. We note that the trajectory of a large body is quite flat in comparison with the one of a small body. It is understood that the inertia effect of a large body, which prevents the body getting off the straight path, predominates over the hydrodynamic interaction force due to the presence of a second body.

For a variety of radius ratios a/b from 0.1 to 1.0 and a fixed density ratio 0.89, the velocity components u and v of the moving cylinder are shown in Fig.9. The initial condition used in the calculation is $x_o = -20$, $y_o = 0.5$, $u_o=1.0$, and $v_o = 0.0$. This plot is consistent with the physical

interpretation. The velocity u is reduced as the moving body approaches the fixed body, and after a certain position, it increases and reaches a maximum value around the top of the stationary cylinder. On the other hand, the velocity v increases from zero to a maximum value in approaching and decreases to zero after the cylinder passes over the fixed one. We also note from Fig.9 that for $x < -2.5$, velocity components for cylinders of different radii are of the same value practically. It indicates that for two bodies apart from each other by a large distance, the hydrodynamic interaction does not have any effects on their motion.

VI. CONCLUSIONS

The hydrodynamic interaction between two circular cylinders of different radii moving relative to each other in a general manner is investigated based on the generalized Taylor's added-mass formula in terms of isolated interior doublets or surface source distributions. The velocity potential of the fluid is expressed in terms of three independent added masses and their derivatives with respect to the separation distance, which are functions of relative sizes of the two cylinders and the separation distance. By extending Hicks' analysis, series expressions have been developed for derivatives of added masses based on the successive image method. In the general case of an oblique impact, it has been found that the numerical evaluation of the derivatives of added masses is more difficult than that of added masses themselves, because of the sensitive dependence of integrals in the integral equations on the separation distance.

The Lagrange's equations of motion governing the motion of a drifting cylinder relative to a stationary one are integrated to obtain the trajectory of the moving cylinder. The numerical results exhibit the dependence of the hydrodynamic interaction force on the direction of the flow with respect to the centerline joining the centers of two cylinders. The velocity component along the centerline produces a repulsive interaction force, which prevents the collision of two bodies, while the component perpendicular to it produces an attractive interaction force. Thus, the collision or non-collision prediction for general oblique motions of two cylinders is much more complicated than that for the central-impact problem.

Due to the limitation of the potential-flow analysis, the afore-mentioned results are only applicable to the situation where the effects of fluid inertia and nonuniformity of the flow due to the presence of a second body are dominant.

REFERENCES

1. Hicks,W.M., "On the Motion of Two Cylinders in a Fluid," Quart. J. Mathematics, Vol. XVI, 1879, 113-140, 193-219.

2. Lamb, H., Hydrodynamics, 6th ed., Chapter 6, Cambridge University Press, U.K., 1932.

3. Yamamoto, T., "Hydrodynamic Forces on Multiple Circular Cylinders," J. Hydr. Div. ASCE, Vol. 102(HY9), 1976, 1193-1210.

4. Isaacson, M. and Cheung, K.F., "Hydrodynamics of Ice Mass near Large Offshore Structure," Waterway, Port, Coastal and Ocean Engineering, Vol. 114, No.4, July 1988,487-502.

5. Hicks,W.M., "On the Motion of Two Spheres in a Fluid," Proc. Trans. Roy. Soc. London, V. 171-II, 1880, 455-492.

6. Landweber, L., Chwang, A.T., and Guo, Z., "Interaction between Two Bodies Translating in an Inviscid Fluid," Submitted to the J. of Ship Research, 1989.

7. Landweber, L. and Chwang, A.T., "Generalization of Taylor's Added-Mass Formula for Two Bodies," J. of Ship Research, Vol. 33, No.1, March 1989, 1-9.

8. Müller, W., "Systeme von Doppelquellen in der ebenen Stromung, insbesondere die Stromung um zwei Kreiszylinder," Zeitschrift fur Angewandte Mathematik und Mechanik, Band 9, Heft 3, June 1929, 200-213.

9. Landweber, L. and Yeh, C.S., "Forces, Moments, and Added Masses for Rankine Bodies," J. of Fluid Mechanics, Vol. 1, 1956, 319-336.

10. Yih, C.S., Fluid Mechanics, Chapter 4, West River Press, 1979.

11. Rouse, H. et. al., Advanced Mechanics of Fluids, Chapter 3, Robert E. Krieger Publishing Company, 1976.

12. Herman, R.A., "On the Motion of Two Spheres in Fluid and Allied Problems," Quart. J. Math,V. 22, 1887, 204-231.

13. Atkinson, K. E., An Introduction to Numerical Analysis, Chapter 5, John Wiley & Sons. Inc., 1978.

Table 1. The Analytic and Numerical Results of Added-Mass Coefficients for Two Circles (a/b = 1.0)

s	k_{11}^e	$-k_{12}^e$	k_{11}^a	$-k_{12}^a$	k_{11}^b	$-k_{12}^b$	k_{11}^c	$-k_{12}^c$	ω^d
2.01	1.3753	0.7283	**.**	**.**	**.**	**.**	1.3713	0.7214	12.0
2.02	1.3416	0.6924	**.**	**.**	1.1650	0.5159	1.3400	0.6901	12.5
2.03	1.3174	0.6661	1.8778	1.2302	1.2843	0.6330	1.3169	0.6653	13.0
2.04	1.2980	0.6446	1.3963	0.7446	1.2893	0.6358	1.2979	0.6443	13.5
2.05	1.2818	0.6262	1.3148	0.6600	1.2791	0.6236	1.2817	0.6261	14.0
2.06	1.2677	0.6100	1.2805	0.6232	1.2668	0.6092	1.2676	0.6100	14.5
2.07	1.2552	0.5955	1.2604	0.6009	1.2549	0.5952	1.2552	0.5955	15.0
2.08	1.2440	0.5822	1.2462	0.5845	1.2439	0.5821	1.2440	0.5822	15.0
2.09	1.2339	0.5700	1.2384	0.5710	1.2338	0.5700	1.2339	0.5700	15.5
2.10	1.2246	0.5587	1.2250	0.5592	1.2246	0.5587	1.2246	0.5587	16.0
10.0	1.0002	0.0200	1.0002	0.0200	1.0002	0.0200	1.0002	0.0200	90.0

superscript: e - exact solution from the method of successive images

a - numerical solution of Eq(34) by the trapezoidal rule with 80 points

b - numerical solution of Eq(37) by the trapezoidal rule with 80 points

c - numerical solution of Eq(37) by the Gaussian quadrature with 60 points

d - ω is measured by degrees

. - solution not convergent within 50 iterations

Table 2. The Analytic and Numerical Results of the Derivatives of Added-mass Coefficients for Two Circles (a/b=1.0 and ω=20°)

s	$\frac{dk_{11}}{ds}\|_e$	$\frac{dk_{11}}{ds}\|_n$	$\frac{dk_{12}}{ds}\|_e$	$\frac{dk_{12}}{ds}\|_n$
2.01	-4.22048	-4.10983	4.43434	4.32371
2.02	-2.77334	-2.77325	2.98604	2.98597
2.03	-2.13769	-2.13769	2.34932	2.34931
2.04	-1.76190	-1.76190	1.97240	1.97240
2.05	-1.50575	-1.50575	1.71691	1.71691
2.06	-1.32129	-1.32129	1.52955	1.52955
2.07	-1.17771	-1.17771	1.38485	1.38485
2.08	-1.06291	-1.06291	1.26892	1.26892
2.09	-0.96858	-0.96858	1.17347	1.17347
2.10	-0.88942	-0.88942	1.09319	1.09319

Subscripts: e - exact solution from the iterative formulas (30) and (31)

n - numerical solution of (43a,b) and (45) by the Gaussian quadrature formula with 160 points

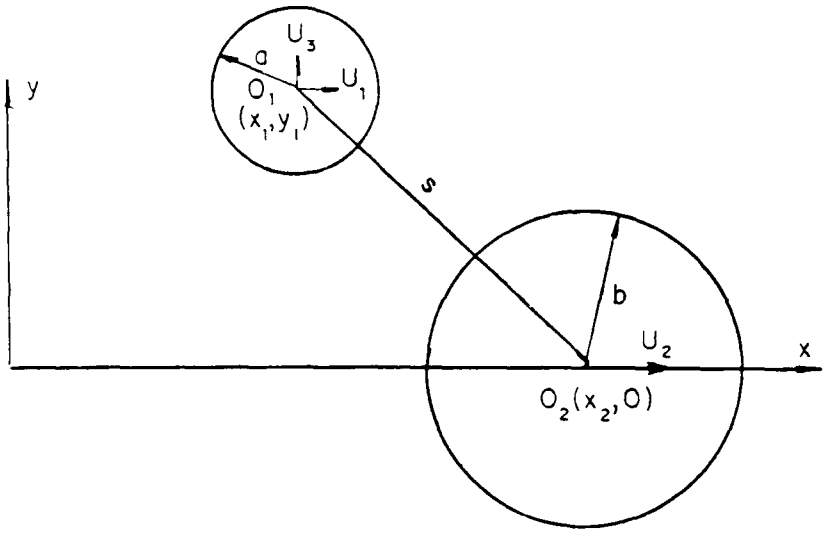

Figure 1a. Relative rectangular coordinate system and velocity components.

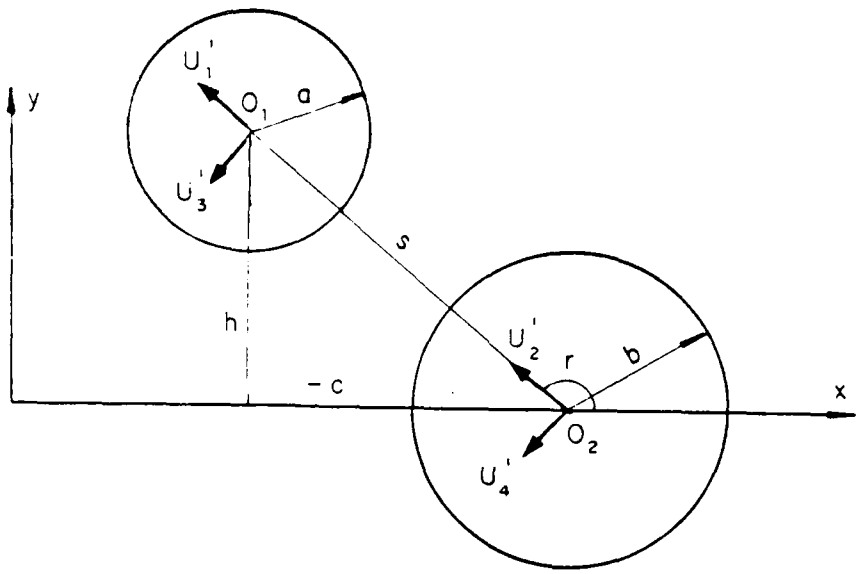

Figure 1b. Relative polar coordinate system and velocity components.

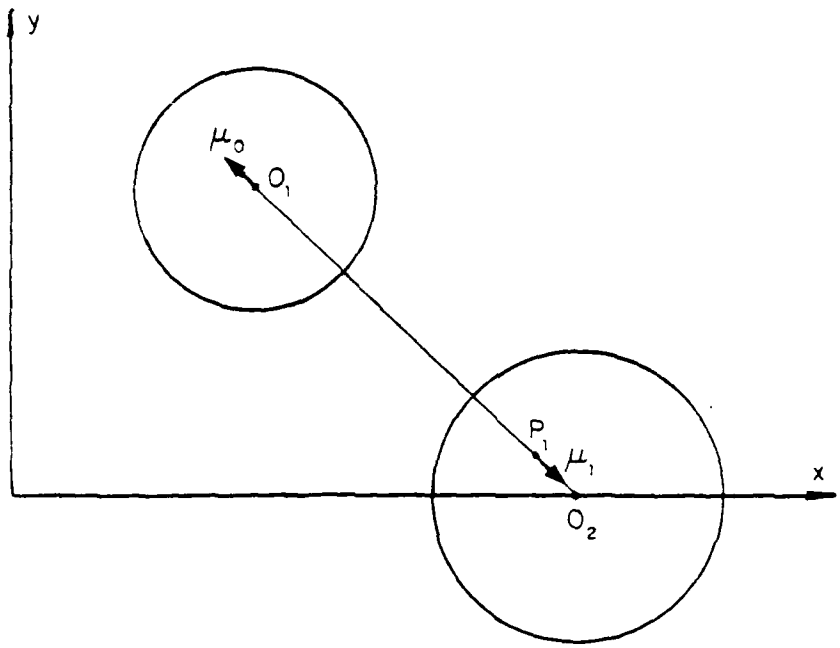

Figure 2. First two images for two circles.

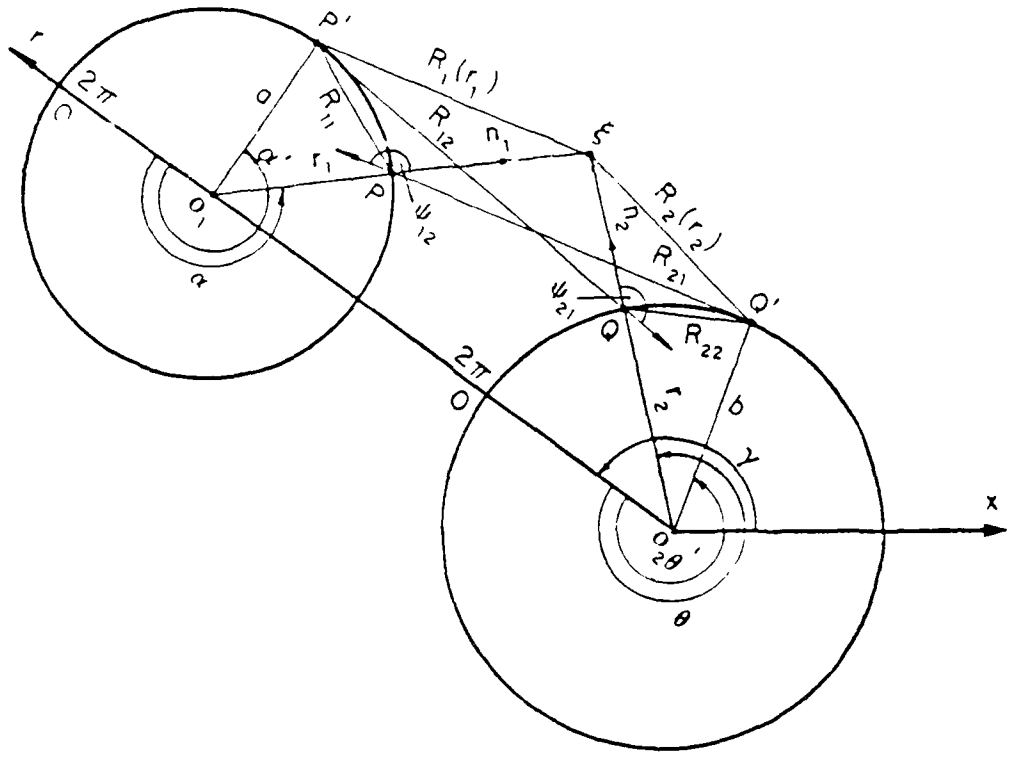

Figure 3a. Surface integration of source distributions on circles 1 and 2.

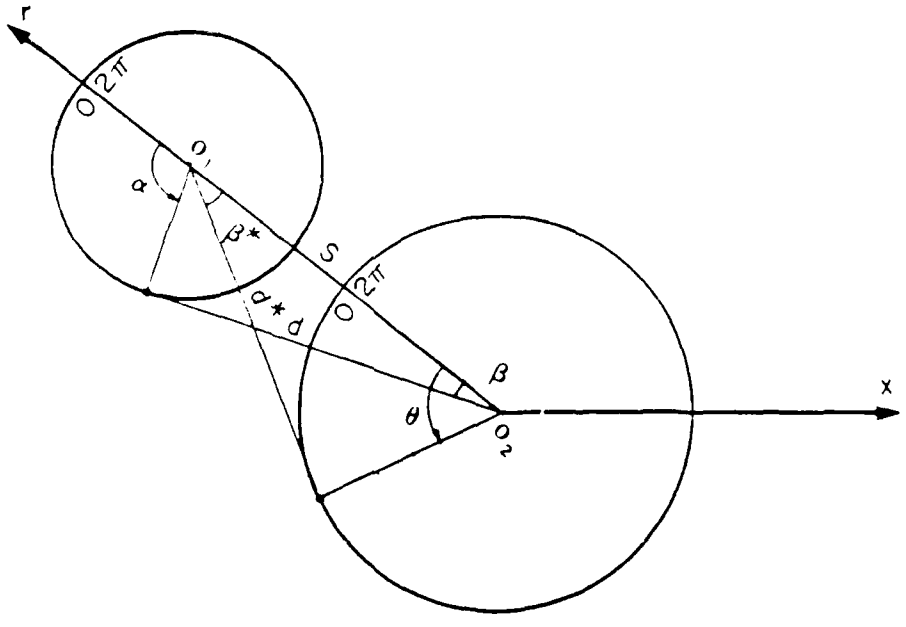

Figure 3b. Definition sketch for d, d*, β, and β* used in equations (40) and (41).

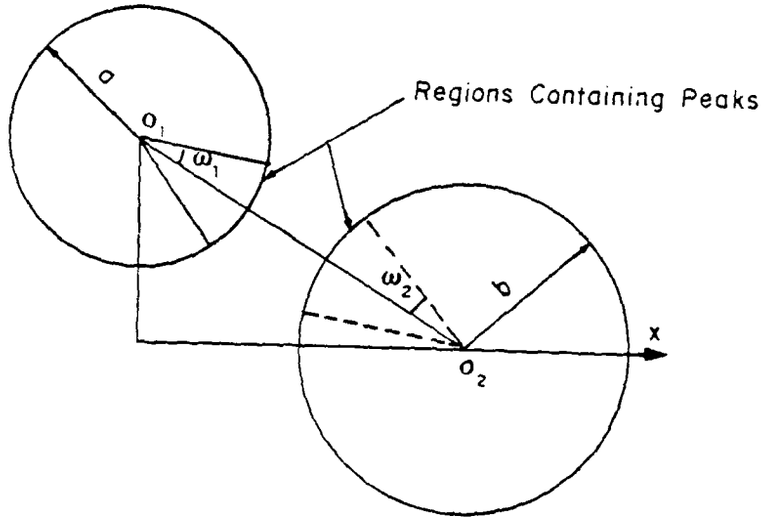

Figure 4. Definition of regions containing peaks.

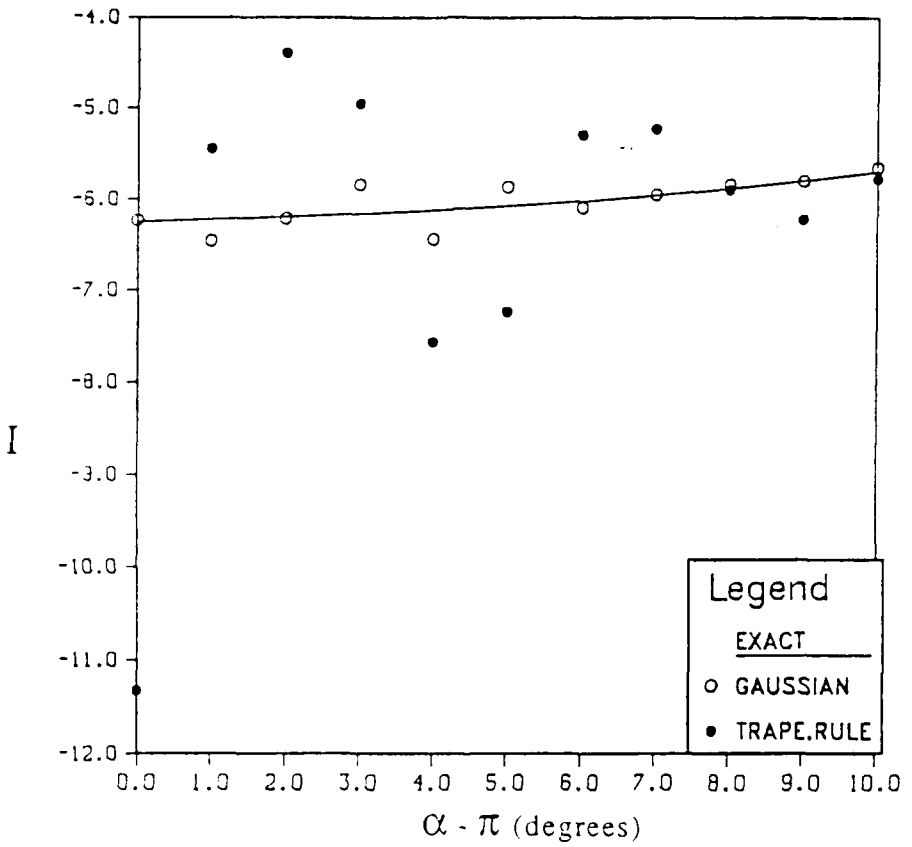

Figure 5. Comparison of numerical results of integral I in equation (42) obtained by the trapezoidal rule with 80 points and by the Gaussian quadrature with 60 points.

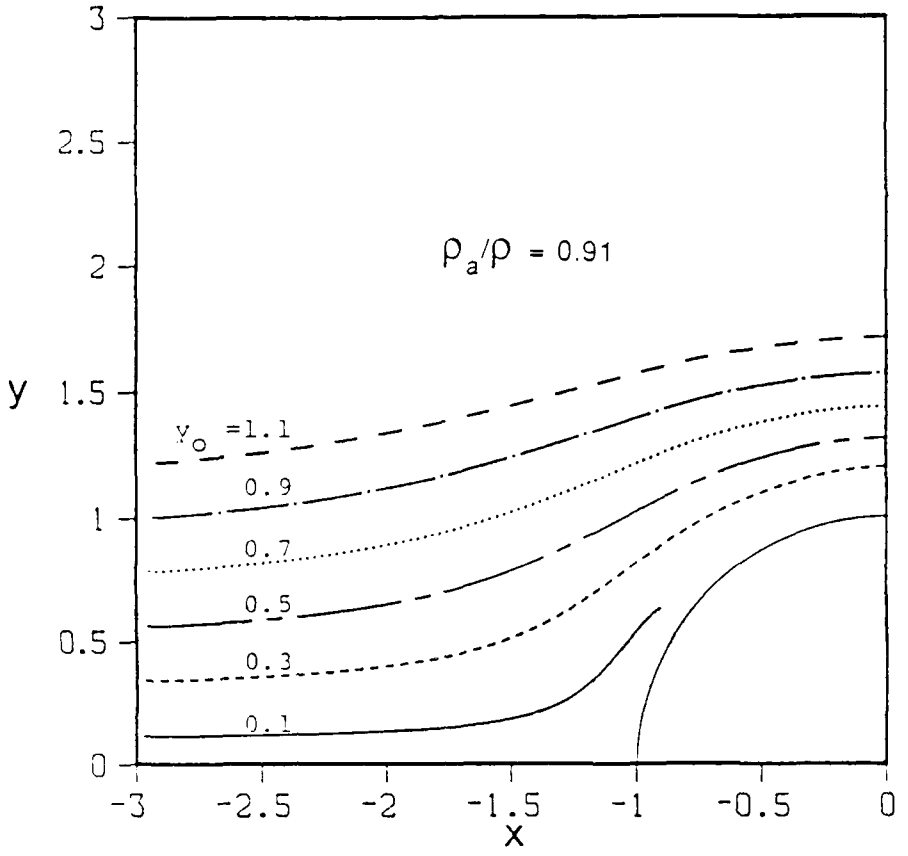
3
2.5
2
1.5
1
0.5
0
y
ρ_a/ρ = 0.91
y_o =1.1
0.9
0.7
0.5
0.3
0.1
-3
-2.5
-2
-1.5
-1
-0.5
0
x

Fig.6(a)

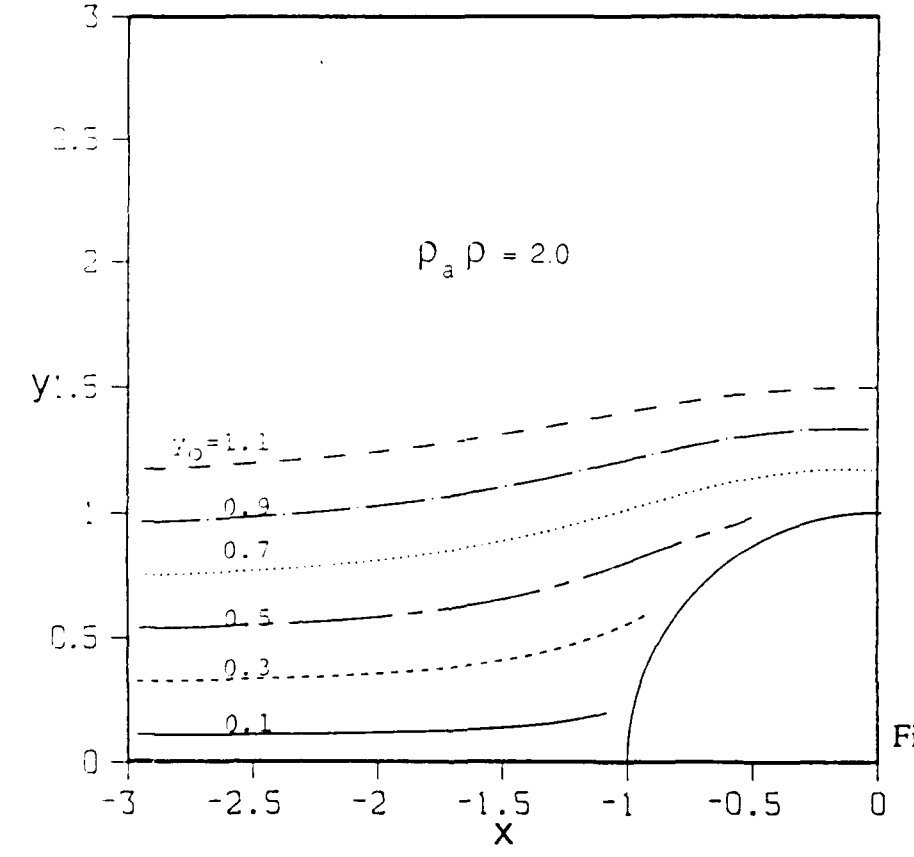
3
2
0.5
0
$\rho_a \rho$ = 2.0
y_o=1.1
0.9
0.7
0.5
0.3
0.1
-3
-2.5
-2
-1.5
-1
-0.5
0
x

Fig.6(b)

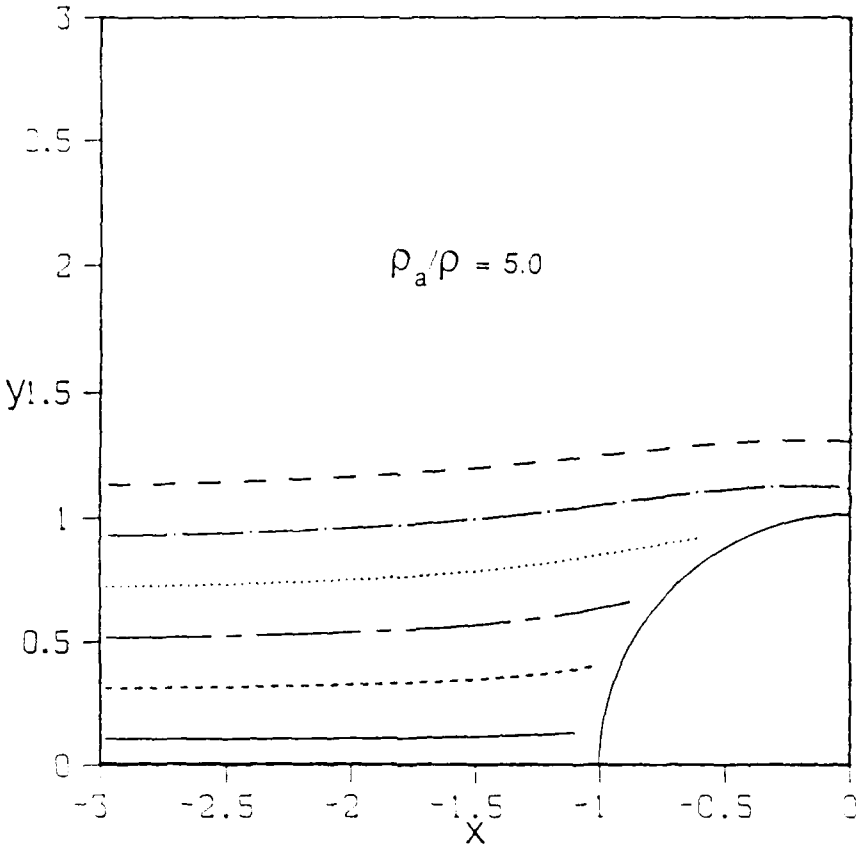
ρ_a/ρ = 5.0
y
x
3
2.5
2
1.5
1
0.5
0
-3
-2.5
-2
-1.5
-1
-0.5
0

Fig.6(c)

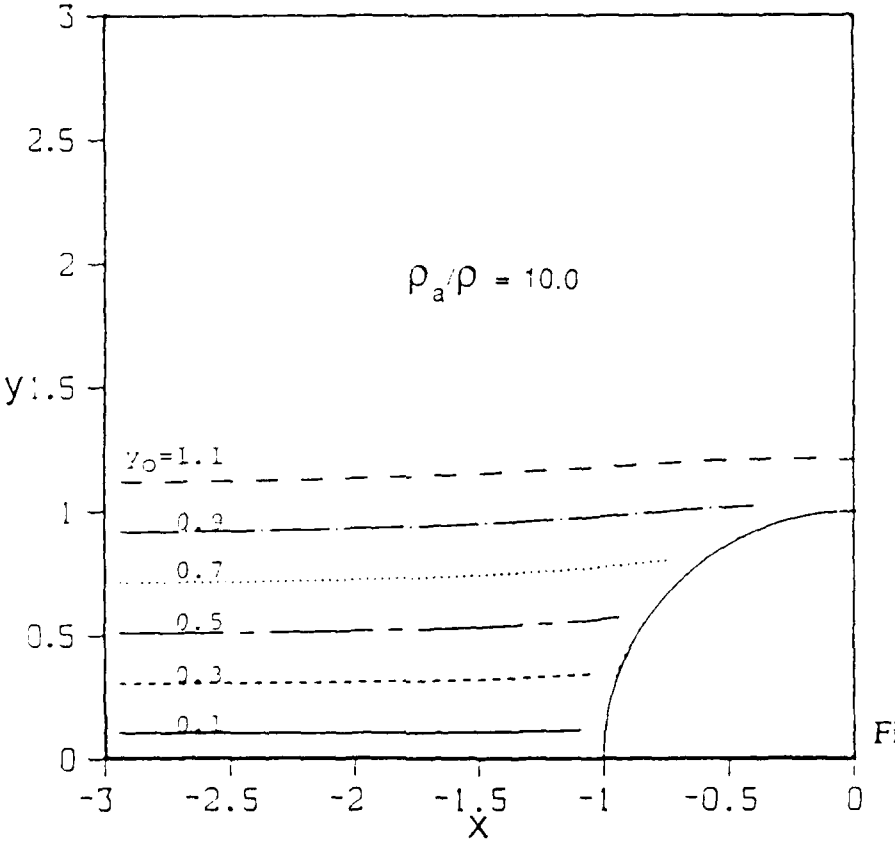
ρ_a/ρ = 10.0
y_0=1.1
0.9
0.7
0.5
0.3
0.1
y
x
3
2.5
2
1.5
1
0.5
0
-3
-2.5
-2
-1.5
-1
-0.5
0

Fig.6(d)

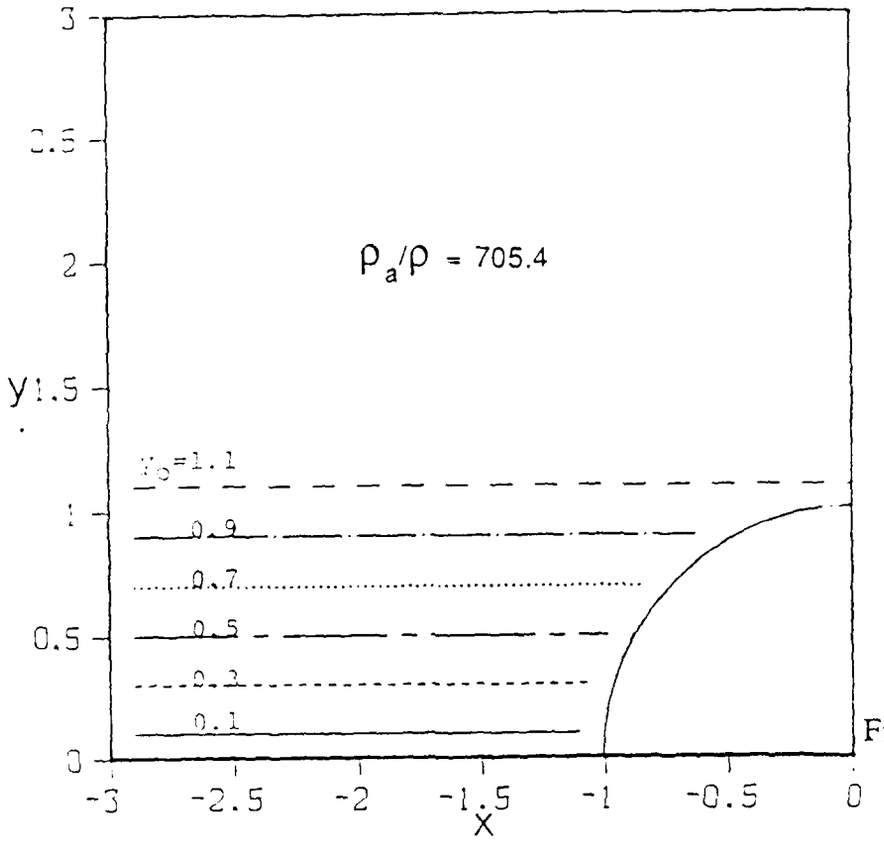

Fig.6(e)

Figure 6. Trajectories of a moving cylinder in different fluids with a/b=0.1, ρ_a = 0.91, U_o = 1.0, and x_o = -20.

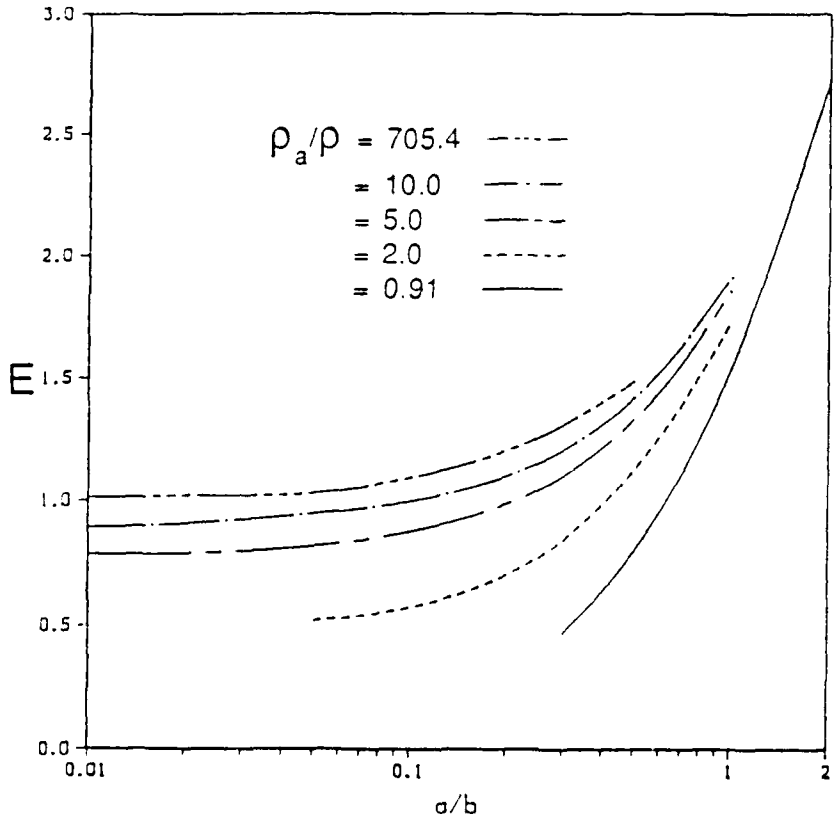

Figure 7. Dependence of the collection coefficient of an ice particle on its size for various density ratios.

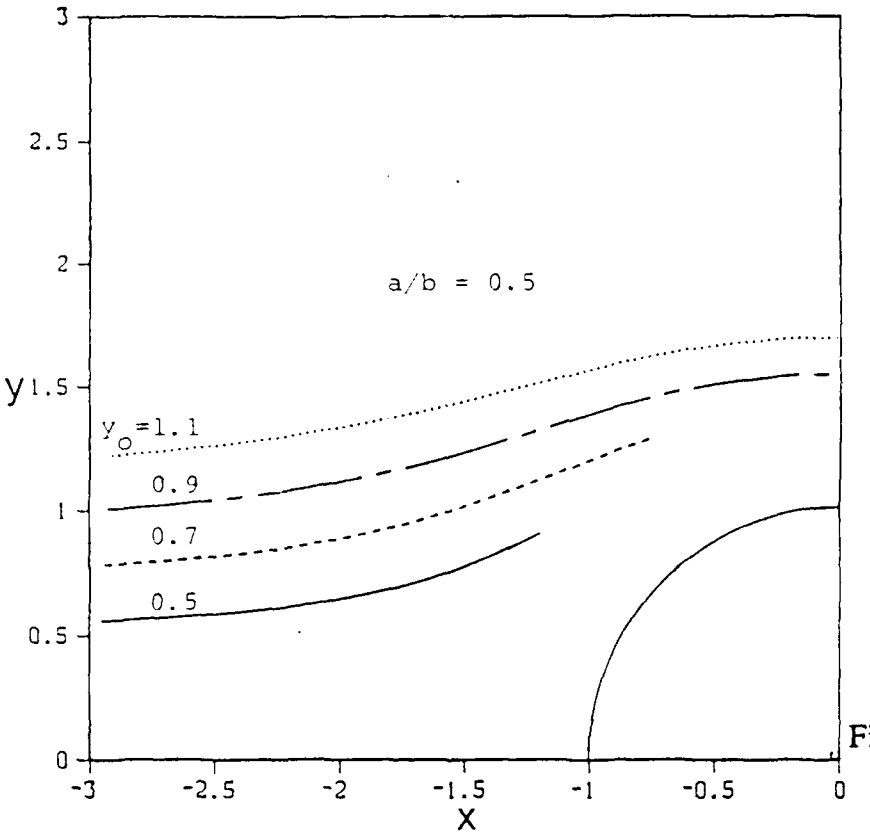

Fig. 8(a)

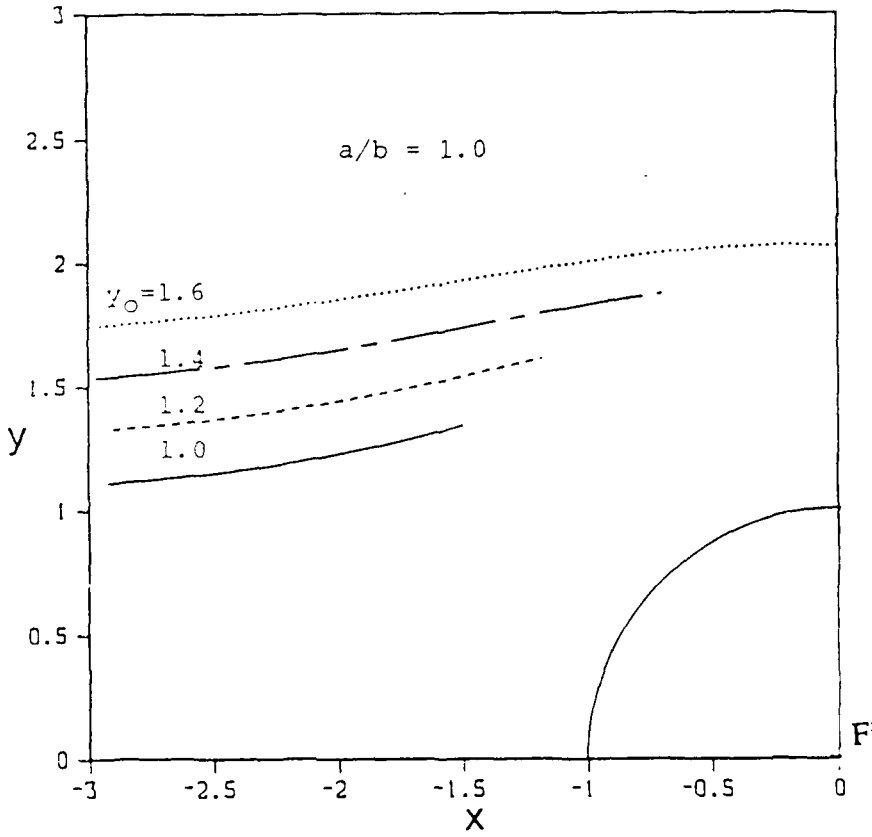

Fig. 8(b)

Figure 8. Trajectories of a moving cylinder with $U_o = 1.0$, $\rho_a = 0.91$, and $\rho_a/\rho = 0.89$.

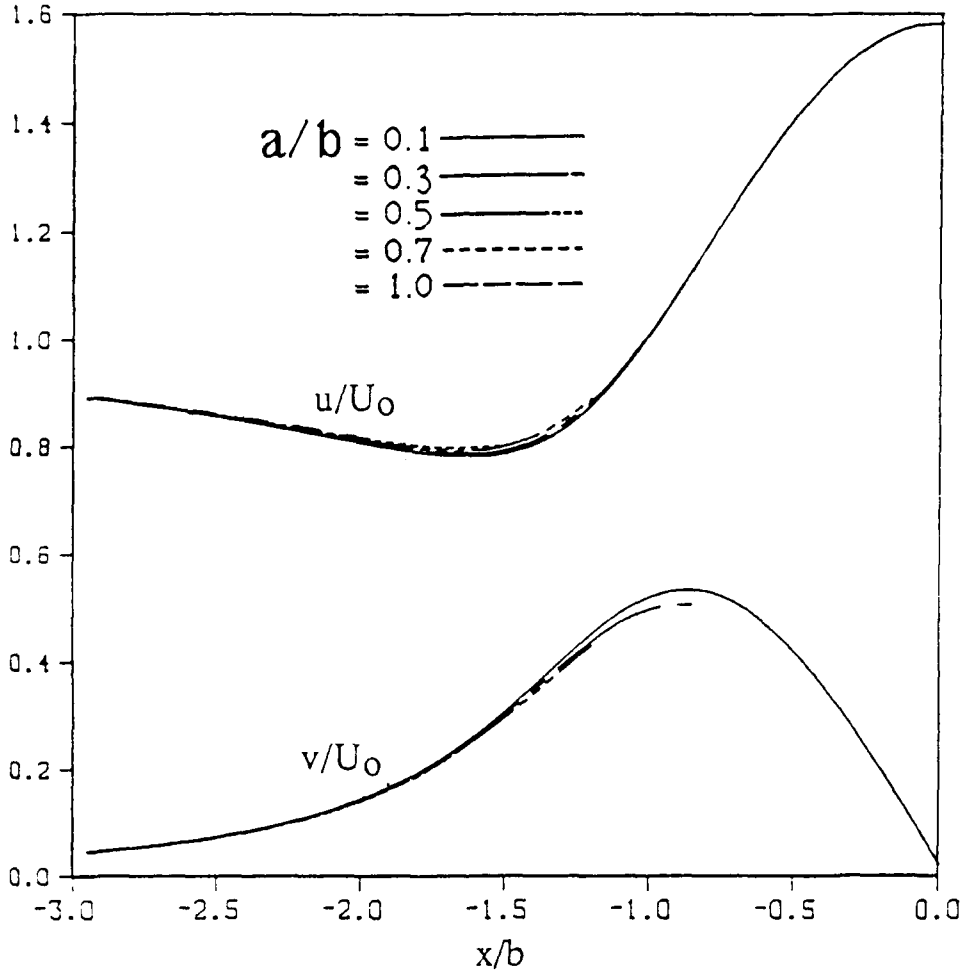

Figure 9. Velocity components u and v of a moving cylinder with various radius ratios.